CROATICA CHEMICA ACTA
CCACAA **80** (3-4) 453–459 (2007)

ISSN-0011-1643
CCA-3188
Original Scientific Paper

Electroacoustic Characterization of Bidisperse Suspensions*

María L. Jiménez,[a] Francisco J. Arroyo,[b] Silvia Ahualli,[a] Raúl Rica,[a] and Ángel V. Delgado[a,]**

[a]*Department of Applied Physics, Faculty of Science, University of Granada, Spain*

[b]*Department of Physics, Faculty of Experimental Science, University of Jaén, Spain*

RECEIVED DECEMBER 19, 2006; REVISED MAY 25, 2007; ACCEPTED JUNE 4, 2007

Electroacoustic techniques are promising tools for the size determination and electrokinetic characterization of concentrated colloidal suspensions. When particles are not homogeneous in size and/or density, the dynamic mobility obtained is a kind of average of the mobilities of every particle. In this paper, we try to discern which averaging procedure provides a better description of the dynamic mobility of bidisperse suspensions consisting of a mixture of two very different types of particles. The results show that the amplitude of the sound wave induced by an applied ac field (electrokinetic sonic amplitude) is not just the sum of the amplitudes of the waves generated by every particle but has a larger contribution from the larger particles, although the small size entities considerably influence the behaviour of the latter because of their interference in the fluxes of the fluid and ions around them.

Keywords
electrokinetics
ESA
polydisperse suspensions
electroacoustics

INTRODUCTION

Concentrated colloidal systems exhibit a wide spectrum of phenomena that have their origin in interactions between particles. Colloidal aggregation, rheological properties, electrorheological and magnetorheological effects,[1–3] anomalous electroorientation of elongated particles,[4] the presence of new phases or phase separation due to depletion in bidisperse systems[5] are some of the new topics of increasing interest to workers in the field.

However, in such concentrated systems, the description of the system by classical techniques, like dynamic light scattering or microelectrophoresis, is essentially useless, since they are based on optical methods. In contrast, the electroacoustic determination of dynamic mobility (the ac counterpart of classical, or dc, electrophoretic mobility) becomes extremely useful to describe the electrical state of the particle/solution interface. Also, this technique provides the dependence of dynamic mobility on the frequency of the external electric field, that is, much more information than that available with a single value such as electrophoretic mobility.

There are two such techniques. One involves the generation of a pressure wave when an ac electric field is applied to the suspension: the amplitude of the sound wave, A_{ESA}, is known as electrokinetic sonic amplitude, and so we speak of the ESA effect. The second method, reciprocal of ESA, is based on the determination of the electric potential induced by the passage of a sound wave through the system. It is called the colloid vibration potential (CVP) or colloid vibration current (CVI) depending on the quantity measured. After the very early works

* Dedicated to Professor Nikola Kallay on the occasion of his 65th birthday.

** Author to whom correspondence should be addressed. (E-mail: adelgado@ugr.es)

on the subject, particularly those by Debye, and Booth and Enderby,[6–9] O'Brien[10,11] carried out an investigation on the physical foundations of electroacoustic techniques, based on the concept of dynamic electrophoretic mobility, u_d^*, a complex quantity that is in fact proportional to the ESA signal, from which it can be derived:[11]

$$A_{ESA} \propto \phi \frac{\Delta\rho}{\rho_m} u_d^* \quad (1)$$

where ϕ is the volume fraction of solids and $\Delta\rho = \rho_p - \rho_m$ is the density contrast, ρ_p (ρ_m) being the density of the particles (dispersion medium). The dynamic mobility u_d^* is the constant of proportionality between the electrophoretic velocity of the particle and the ac electric field, at zero pressure gradient.

In this work, we analyze the way how to use the dynamic mobility of bidisperse systems for their electrokinetic characterization. In Ref. 12, the authors demonstrated that in the case of homogeneous mixtures, we would expect a kind of average value between the mobilities of both particles. However, as we will see, such a law is obeyed only in the case of slight polydispersity.

Theoretical Background

Charged colloidal particles in aqueous suspensions migrate under the action of an electric field. The forces acting on each particle are of electric and viscous origin, and come, basically, from the action of the external field on the particle's charge, the viscous friction with the fluid (also in motion because of the effect of the field on the charged double layer), and, eventually, the local field generated by the polarized double layer. To this we must add the hydrodynamic and electrical interactions between particles, if their concentration is large enough. An approximate formula accounting for these effects is:[13–15]

$$u_d^* = \frac{2}{3} \frac{\varepsilon_0 \varepsilon_m \zeta}{\eta} (1 - C^*)\, G^* \quad (2)$$

where ζ is the zeta potential, η the viscosity of the medium, ε_0 the vacuum permittivity, ε_m the relative permittivity of the medium, and C^* the induced dipole coefficient related to the induced dipole $\vec{d}$ by the expression:

$$\vec{d} = 4\pi\varepsilon_0\varepsilon_m a^3 [C_1 - iC_2] \vec{E}_0 \quad (3)$$

where a is the particle radius and C_1 and C_2 are the real and imaginary parts of C^*. In Eq. (2), G^* is the complex function that accounts for the particle and fluid inertia in the presence of an applied field of frequency ω given by:

$$G^* = \frac{1+\lambda}{1+\lambda+\frac{\lambda^2}{9}\left(3+2\frac{\Delta\rho}{\rho_m}\right)} \quad (4)$$

In this expression,

$$\lambda = (1+i)\sqrt{\frac{\omega a^2 \rho_m}{2\eta}} \quad (5)$$

corresponds to the product ka, where k is the complex wave vector of the fluid velocity wave provoked by the oscillations of particles in the viscous liquid under the action of the external electric field.[16] It must be noted that Eq. (2) is only valid if the particle size a is much larger than the double layer thickness, given by the Debye length κ^{-1}:

$$\kappa^{-1} = \sqrt{\frac{k_B T \varepsilon_0 \varepsilon_m}{\sum_{i=1}^{N} z_i^2 e^2 n_i^\infty}} \quad (6)$$

where N is the total number of ionic species in the medium, $z_i e$ is the charge of the i-th ion and n_i^∞ its bulk number concentration, k_B the Boltzmann constant and T the absolute temperature. Recall that the so-called thin double layer approximation is usually written as $\kappa a > 1$.

Hence, in the first approximation, the dynamic electrophoretic mobility will be determined by the zeta potential, and both the dipole coefficient and inertia factor at each frequency.

Recall that if an alternating electric field is applied, the dipole coefficient depends on its frequency because of the different time scales of the various phenomena that contribute to the induced dipole. Hence, like, for instance, the permittivity of the suspension, dynamic mobility will exhibit one or more relaxation phenomena, in addition to the high-frequency decline, always present because of

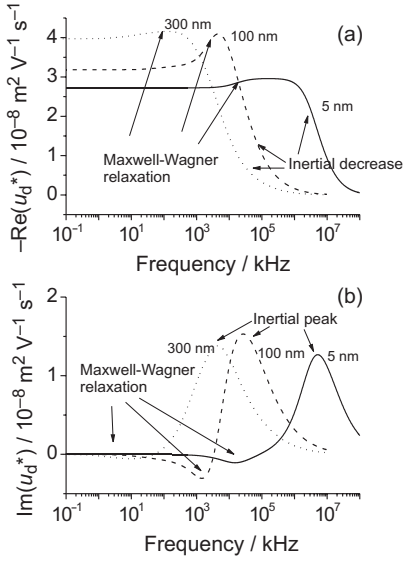

Figure 1. Real (a) and imaginary (b) parts of the dynamic mobility of a suspension of spherical particles in 0.5 mmol dm^{-3} KCl, with ϕ = 1 %, ζ = –100 mV and the particle radii indicated.

inertia. For example, in Figure 1 we plot the real (a) and the imaginary part (b) of the mobility of an aqueous suspension of spherical particles.[13,17]

The curves corresponding to different particle radii show well defined increases (at low frequencies) and decreases (high frequencies), with characteristic frequencies clearly dependent on the size, and very easy to observe in the imaginary component of the mobility u_d^* (part (b)) of Figure 1. The low-frequency raise is associated with the Maxwell-Wagner-O'Konski (MWO) relaxation of the induced dipole:[18–19] below the characteristic frequency, the different conductivities of the particle and solution provoke accumulation of counterions on one side of the particle, and depletion on the opposite side, thus producing a contribution to the dipole. If the frequency is increased above that value, the ionic electromigration does not have time to occur, and the dipole coefficient decreases, *i.e.*, the modulus of the mobility increases. The characteristic frequency of this MWO relaxation is:

$$\omega_{MWO} = \frac{(1-\phi)\kappa_p + (2+\phi)\kappa_m}{(1-\phi)\varepsilon_p\varepsilon_0 + (2+\phi)\varepsilon_m\varepsilon_0} \qquad (7)$$

where ϕ is the volume fraction of solids, κ_p and κ_m are the conductivity of the particle and solution, respectively, and ε_p is the dielectric constant of the particle. For the case of insulating particles with a charged interface, this equation can be still used after substituting κ_p by the effective conductivity of a particle plus its ionic atmosphere due to the excess of ions in the EDL ($\kappa_p = 2\kappa^\sigma / a$ for $\kappa a >> 1$ and $\kappa_p = 2\kappa^\sigma / \kappa^{-1}$ for $\kappa a < 1$, where κ^σ is the surface conductivity of the EDL[19]).

As mentioned, for high enough frequencies, the mobility decreases due to the inertia of the particle. If this is small enough (solid and dashed lines in Figure 1), this decrease is well separated from the MWO relaxation. In this case, we can expect an increase of the mobility modulus followed by inertial decay (Figure 1a). Accordingly, the imaginary part of u_d^* should exhibit two peaks (Figure 1b). However, for colloids a few hundred nanometers in size (dotted line in Figure 1), the Maxwell-Wagner relaxation will be hidden by inertial decay.

As regards concentrated systems, the model has to be dramatically changed because we have to consider the hydrodynamic interactions between particles and, if the double layers overlap, also their electrical interactions. This problem is usually overcome by means of cell models,[20,21] where the suspension is substituted by a single particle surrounded by a finite shell of electrolyte, and with some appropriate boundary conditions for the electric and hydrodynamic problems. Details of the model can be found in Refs. 13, 22, and 23. The important results are: (*i*) the mobility decreases with the volume fraction of solids ϕ; (*ii*) both the Maxwell-Wagner relaxation and the inertial decrease take place at higher frequencies when we increase ϕ, and (*iii*) the amplitude of the Maxwell-Wagner relaxation decreases under the same conditions.

EXPERIMENTAL

The suspensions were composed of two kinds of particles: UCM190 polystyrene spheres and A300 silica spheres (aerosil A300, Degussa-Hüls AG) both negatively charged. Their sizes and electrophoretic mobilities (classical or DC, u_e) are detailed in Table I. The size was obtained from transmission electron microscope pictures. The mobilities were measured in a Malvern Zetasizer 2000 (Malvern Instruments, England). Dynamic mobility was determined by the Electroacoustic Sonic Amplitude (ESA) technique, using an AcoustoSizer II (Colloidal Dynamics, USA). In this device, the particles vibrate under the action of an oscillating electric field generating a sonic wave, whose amplitude (A_{ESA}) is given by Eq. (1). In the case of our bidisperse systems, we used an average density contrast and the total volume fraction of solids as input data. The method is particularly suitable for evaluation of the electrokinetic properties of concentrated colloidal suspension.[6,24]

All experiments were carried out at 25 °C.

RESULTS

Figure 2 displays the experimental results obtained for the suspensions of UCM190 latex particles, and two salt concentrations. The size and zeta potential of the particles are such that the MWO relaxation (increase in $\mathrm{Re}(u_d^*)$ and minimum in $\mathrm{Im}(u_d^*)$ are clearly observed for the two KCl concentrations, while the inertial fall (and its corresponding maximum in $\mathrm{Im}(u_d^*)$ is just suggested by the experimental data, considering the frequency range accessible to the instrument (ν = 1–18 MHz). Interestingly, the cell model[13] (lines in Figure 2) is capable of describing the results with high accuracy. Table II displays the zeta po-

TABLE I. Identification of the particles used, together with their radii and dc electrophoretic mobilities u_e in 0.5 mmol dm^{-3} KCl solutions

Particle	Radius / nm	u_e / 10^{-8} m^2 V^{-1} s^{-1}
UCM190	168	–4.3
A300	7.0	–2.5

TABLE II. Zeta potential for the best fit of the model of Ref. 13 to the experimental results of dynamic mobility of the suspensions indicated

Suspension	ζ / mV
UCM190 4.77 % + 0.1 mmol dm^{-3} KCl	–200
UCM190 4.77 % + 0.5 mmol dm^{-3} KCl	–150
A300 5.22 % + 0.5 mmol dm^{-3} KCl	–16

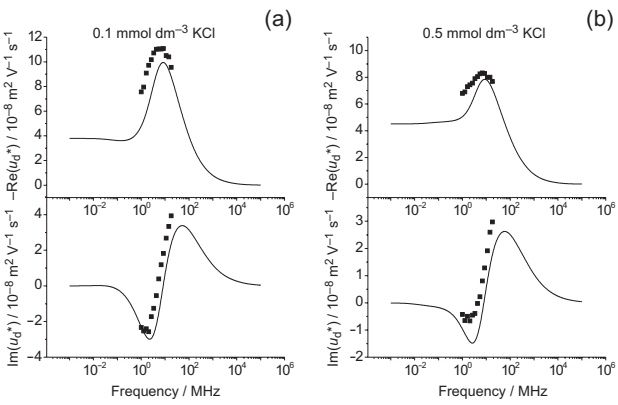

Figure 2. Real and imaginary parts of the dynamic mobility of the suspension UCM190 4.77 %, 0.1 mmol dm^{-3} KCl (a) and 0.5 mmol dm^{-3} KCl (b). Solid lines are the best fit of the cell model of Ref. 13, using the zeta potential as a fitting parameter (Table II) and the radius deduced from TEM pictures.

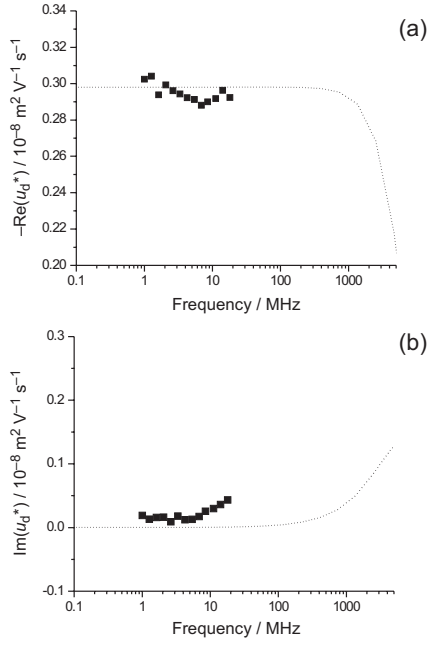

Figure 3. Real (a) and imaginary (b) parts of the dynamic mobility of the suspension A300 5.22 %, 0.5 mmol dm^{-3} KCl. Lines are the best fit of the cell model of Ref. 13.

tentials required to get such a good proximity between theory and experiment.

Figure 3 shows the experimental results for suspensions of A300. In this case, no Maxwell-Wagner effect is observed, since the particles are very small, and, in addition, the characteristic frequency of the inertial decrease is beyond the frequency range available. Because of this (and also because of the high probability of aggregation between such small particles), the cell model does not provide an accurate description of the data if we use the TEM particle radius (Table I) and the best-fit zeta potential given in Table II.

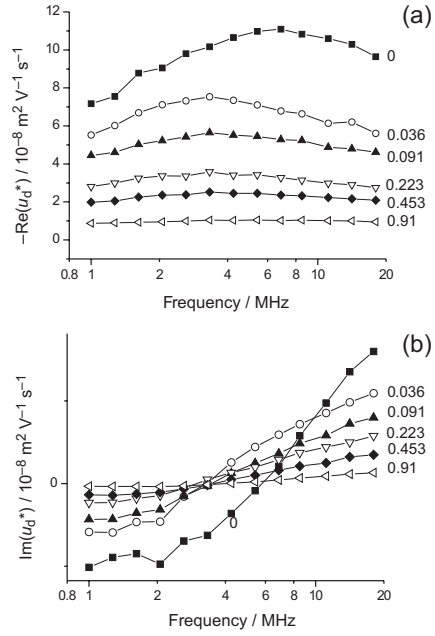

Figure 4. Real (a) and imaginary (b) parts of the dynamic mobility of the suspension UCM190 4.77 % and 0.1 mmol dm^{-3} KCl, and the concentrations (% volume fraction) of A300 indicated in the Figure.

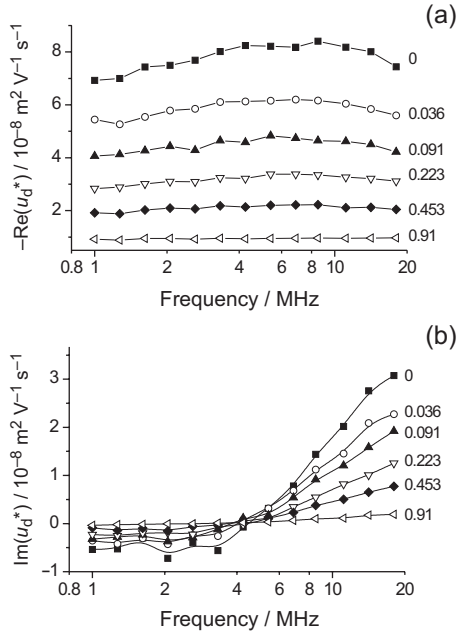

Figure 5. The same as Figure 4 but for 0.5 mmol dm^{-3} KCl.

Figures 4 and 5 present the real and imaginary parts of the mobility of UCM190 suspensions (always with 4.77 % volume fraction) with different added concentrations of A300, for KCl 0.1 mmol dm^{-3} (Figure 4) and KCl 0.5 mmol dm^{-3} (Figure 5). As observed, upon addition of even small amounts of aerosil, the mobility decreases sharply, approaching the values corresponding to pure aerosil suspensions. The MWO relaxation reported

in Figure 2 for UCM190 disappears, and the inertial decrease is greatly reduced. The effect is more evident for KCl 0.1 mmol dm^{-3}, where even the position of the inertial peak changes (see Figure 4b).

DISCUSSION

Let us first consider the effect of ionic strength on the dynamic mobility of our suspensions. Figure 2 (corresponding to latex particles alone) allows the observation of the main features of this effect. Increasing the ionic strength reduces the amplitude of the MWO relaxation, and shifts its characteristic frequency to higher values. This frequency change is immediately explained by the dependence of ω_{MWO} on κ_m displayed in Eq. (7). Concerning the amplitude of the relaxation, it must be recalled that increasing the ionic strength brings about a larger accumulation of positive ions on the left side of the particle and of negative ones on its right side (for a field directed from left to right). This tends to make the induced dipole coefficient more negative, and hence closer to its high frequency value Re(C^*) = –1/2. This proximity of low and high frequency values of the dipolar coefficient renders the MWO amplitude smaller.

In the case of mixed suspensions, Figures 4 and 5, corresponding, respectively, to 0.1 mmol dm^{-3} and 0.5 mmol dm^{-3} KCl, demonstrate that such features, although observable, are considerably hidden by the addition of aerosil because of negligible variations of its dynamic mobility with frequency. Nevertheless, for aerosil concentrations below 0.91 %, the shift of the MWO characteristic frequency to higher values as well as the flattening of the frequency dependence of the mobility can be seen when the concentration of KCl is changed from 0.1 mmol dm^{-3} to 0.5 mmol dm^{-3}.

However, the key point of our investigation is the understanding of the effects that the addition of A300 provokes on the dynamic mobility of suspensions. In order to rule out the simple influence of the predominance of one type of particles over the other, we will compare our mobility determinations in mixed suspensions containing (*a* % UCM190 + *b* % A300) with systems containing *b* % A300 (*b* between 0.452 and 1.79). The results are shown in Figure 6 for two KCl concentrations (0.1 mmol dm^{-3} and 0.5 mmol dm^{-3}). Strikingly, in the case of mixtures, the presence of UCM190 is almost completely masked by the A300 silica, even though the volume fraction of the latter is smaller, and its zeta potential lower. Not only the absolute values of the mobility approach the A300 mobility, but also the Maxwell-Wagner effect disappears, like in the A300 spectrum (see Figure 3). The phenomenon is more evident the larger the concentration of A300.

Recall that in polydisperse systems the ESA signal is weighted by both the density contrast and concentration of the particles. If we assume that the ESA signal is a superposition of the individual sonic waves generated by every kind of particle, then the total signal will be:

$$A_{ESA} \propto \int_0^\infty u_d^*(D)\phi(D)\frac{\Delta\rho(D)}{\rho_m}\mathrm{d}D \qquad (8)$$

where D is the diameter, $u_d^*(D)$ is the dynamic mobility of particles with diameter D, $\phi(D)$ is their concentration, and $\Delta\rho(D)$ is their corresponding density contrast. If we

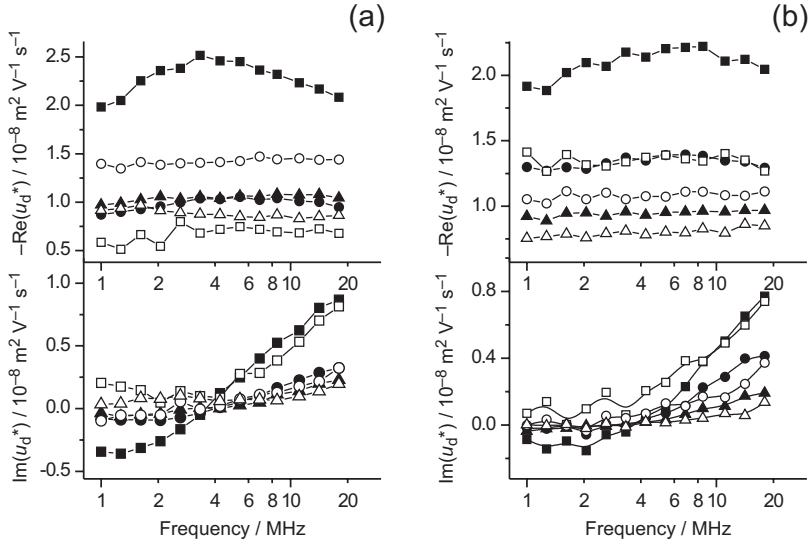

Figure 6. Real and imaginary parts of the dynamic mobility of the mixtures of UCM190 4.77 % and different concentrations of A300 (full symbols) and of the suspensions of A300 alone at the same concentrations (open symbols) always in 0.1 mmol dm^{-3} KCl (a) and 0.5 mmol dm^{-3} KCl (b) A300 concentrations: 0.452 % (■: mixture; □: aerosil alone); 0.910 % (●: mixture, ○: aerosil); 1.79 % (▲: mixture; △: aerosil).

restrict ourselves to the case of a bidisperse suspension, then, taking into account Eqs. (1) and (8):

$$A_{\mathrm{ESA}} \propto \left\langle u_{\mathrm{d}}^{*} \right\rangle \frac{\langle \Delta\rho \rangle}{\rho_{\mathrm{m}}} \phi = \frac{u_{\mathrm{U}}^{*} \phi_{\mathrm{U}} \Delta\rho_{\mathrm{U}} + u_{\mathrm{A}}^{*} \phi_{\mathrm{A}} \Delta\rho_{\mathrm{A}}}{\rho_{\mathrm{m}}} \qquad (9)$$

and the effective dynamic mobility of the mixture will be given by:

$$\left\langle u_{\mathrm{d}}^{*} \right\rangle = \frac{u_{\mathrm{U}}^{*} \phi_{\mathrm{U}} \Delta\rho_{\mathrm{U}} + u_{\mathrm{A}}^{*} \phi_{\mathrm{A}} \Delta\rho_{\mathrm{A}}}{\langle \Delta\rho \rangle \phi} \qquad (10)$$

where the subscript indicates the UCM190 particles (U) and A300 particles (A).

Accordingly, a possible approach to evaluation of the effective dynamic mobility involves using Eq. (10), inserting in it the dynamic mobilities of the individual particles. Since such mobilities depend on the concentration of particles in the medium, the use of Eq. (10) would require knowing the mobility of every particle in its actual environment in the experimental system, but of course we do not have experimental access to it. Hence, the first approximation is to consider that the concentration effect is independent of the kind of particles that surround a given one: for instance, the UCM190 particles are assumed to have the same mobility in a mixture (4.77 % UCM190 + 0.452 % A300) as in a suspension 5.22 % UCM190 (*i.e.*, the total volume fraction of the mixture). With this assumption, and using Eq. (10), we have constructed the theoretical predictions shown in Figure 7. In this figure, we compare the experimental u_{d}^{*} for mixtures 4.77 % UCM190 + 0.452 % A300 (full squares) with the theoretical predictions of Eq. (10) using the following for the individual mobilities of each type of particles:

$$\begin{cases} u_{\mathrm{U}}^{*}: \text{Experimental mobility of UCM190 with } \phi = 4.77\,\% \\ u_{\mathrm{A}}^{*}: \text{Experimental mobility of A300 with } \phi = 0.452\,\% \end{cases}$$

This choice corresponds to the open circles in Figure 7. If we assume:

$$\begin{cases} u_{\mathrm{U}}^{*}: \text{Experimental mobility of UCM190 with } \phi = 5.22\,\% \\ u_{\mathrm{A}}^{*}: \text{Experimental mobility of A300 with } \phi = 5.22\,\% \end{cases}$$

the result is given by the open squares in Figure 7. It is clear that none of the averaging procedures is capable to accurately reproduce the dynamic mobility of the systems. Nevertheless, the closest approach between the experimental data and the estimated averaged mobility is obtained when the mobility of each kind of particle participates in Eq. (10) as if the other particles were absent. In addition, Figure 7 shows that the weight of the larger particles on the average mobility is greater than estimated by the simple mixture formula. We can conclude, in agreement with previous works on similar suspensions,[25,26] that the mixture does not behave as the superposition of the two components, but rather that the behaviour of the system is mostly dominated by the larger colloidal entities, while the role of the smaller particles is to perturb the fluid and ionic flows around the large ones. Hence, the significant effect that, according to Figure 6, the silica particles have on the dynamic mobility of the bidisperse systems must be a consequence of their influence on the non-equilibrium double layer structure of the latex particles in the presence of the field.

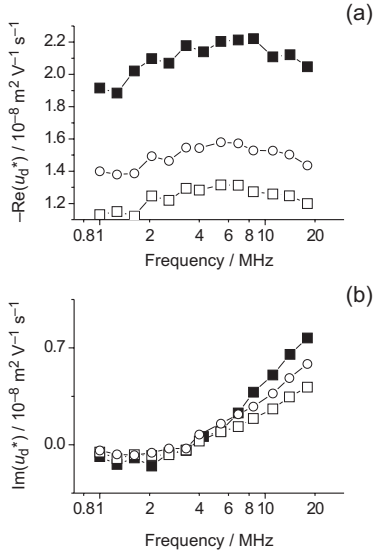

Figure 7. Real (a) and imaginary (b) parts of the dynamic mobility of the mixture of UCM190 and A300. ■: Experimental data for the mixed suspension containing UCM190 4.77 % and A300 0.452 %; ○: Theoretical predictions of the mixture formula Eq. (10) using the experimental data of the single components UCM190 4.77 % and A300 0.452 %; □: Theoretical predictions of the mixture formula Eq. (10) using the experimental data of the single components UCM190 5.22 % and A300 5.22 %.

CONCLUSIONS

In this work, an evaluation has been carried out of the dynamic mobility of bidisperse suspensions consisting of 168 nm latex particles and 7 nm silica particles. Our results indicate that silica has a very significant effect on the electrokinetic behaviour of mixed systems. Comparison between experimental data and different evaluations of the average mobility suggest that this important influence is due to the perturbation of fluid and ionic flows around large particles due to the presence of small particles, and it cannot be explained by a simple superposition of the mobilities of the two populations.

Acknowledgments. – The senior author, A. V. D., is honoured by the invitation to contribute this manuscript to the Festschrift dedicated to Professor N. Kallay. We all wish him a long and fruitful scientific career. Financial support to this work by MEC (Spain) (Projects FIS2005-06860-C02-01, 02) and Junta de Andalucia (Spain) (Projects FQM410) is gratefully acknowledged. Sample UCM190 is a kind gift from Professor E. Enciso, Universidad Complutense de Madrid, Spain.

REFERENCES

1. T. Hao, *Adv. Colloid Interface Sci*. **97** (2002) 1–35.
2. M. J. Espin, A. V. Delgado, and F. González-Caballero, *Phys. Rev. E* **73** (2006) 041503.
3. R. Stanway, *Mater. Sci. Technol*. **20** (2004) 931–939.
4. S. P. Stoylov, *Adv. Colloid Interface Sci*. **50** (1994) 51–78.
5. H. N. W. Lekkerkerker, W. C. K. Poon, P. N. Pusey, A. Stroobants, and P. A. Warren, *Europhys. Lett*. **20** (1992) 559–564.
6. R. J. Hunter, *Colloids Surf., A* **141** (1988) 37–66.
7. R. J. Hunter and R. W. O'Brien, *Electroacoustics,* in: P. Somasundaran and A. T. Hubbard (Eds.), *Encyclopedia of Surface and Colloid Science*, Marcel Dekker, New York, 2005, pp. 2000–2016.
8. J. A. Enderby, *Proc. R. Soc. Lond., Ser. A* **207** (1951) 329–342.
9. F. Booth and J. A. Enderby, *Proc. Phys. Soc.* **65** (1952) 321–324.
10. R. W. O'Brien, *J. Fluid Mech*. **190** (1988) 71–86.
11. R. W. O'Brien, *J. Fluid Mech*. **212** (1990) 81–93.
12. A. S. Dukhin, V. N. Shilov, H. Ohshima, and P. J. Goetz, *Langmuir* **16** (2000) 2615–2620.
13. F. J. Arroyo, F. Carrique, S. Ahualli, and A. V. Delgado, *Phys. Chem. Chem. Phys*. **6** (2004) 1446–1452.
14. A. S. Dukhin, H. Ohshima, V. N. Shilov, and P. J. Goetz, *Langmuir* **15** (1999) 3445–3451.
15. A. S. Dukhin, V. N. Shilov, H. Ohshima, and P. J. Goetz, *Langmuir* **15** (1999) 6692– 6706.
16. L. D. Landau and E. M. Lifshitz, *Fluid Mechanics*, Pergamon, Oxford, 1966, Ch. II–24.
17. F. Carrique, F. J. Arroyo, and A. V. Delgado, *J. Colloid Interface Sci.* **252** (2002) 126–137.
18. J. C. Maxwell, *Electricity and Magnetism*, Vol. 1, Dover, New York, 1954, pp. 452–461.
19. C. T. O'Konski, *J. Phys. Chem.* **64** (1969) 605–619.
20. S. Kuwabara, *J. Phys. Soc. Jpn*. **14** (1959) 527–532.
21. J. Happel, *AIChE J*. **4** (1958) 197–201.
22. V. N. Shilov, N. I. Zharkikh, and Y. B. Borkovskaya, *Colloid J. USSR* **43** (1981) 434–438.
23. A. V. Delgado, S. Ahualli, F. J. Arroyo, and F. Carrique, *Colloids Surf., A* **267** (2005) 95–102.
24. A. S. Dukhin, V. N. Shilov, H. Ohshima, and P. J. Goetz, *Electroacoustic Phenomena in Concentrated Dispersions: Theory, Experiment, Applications*, in: A. V. Delgado (Ed.), *Interfacial Electrokinetics and Electrophoresis, Surfactant Science Series*, Vol. 106, Marcel Dekker, New York, 2002, pp. 493–519.
25. F. Mantegazza, M. Caggioni, M. L. Jiménez, and T. Bellini, *Nat. Phys.* **1** (2005) 103–106.
26. M. L. Jiménez, F. J. Arroyo, A. V. Delgado, F. Mantegazza, T. Bellini, and R. Rica, *J. Colloid Interface Sci*. **309** (2007) 296–302.

SAŽETAK

Elektroakustična karakterizacija bidisperznih suspenzija

María L. Jiménez, Francisco J. Arroyo, Silvia Ahualli, Raúl Rica i Ángel V. Delgado

Elektroakustičke tehnike su vrlo korisne za određivanje veličine i elektrokinetičku karakterizaciju koncentriranih koloidnih suspenzija. Kada čestice nisu homogene po veličini i/ili gustoći, dobivena dinamička pokretljivost je neka vrsta prosjeka pokretljivosti svih čestica. U radu se pokušalo razlučiti koji postupak uprosječivanja najbolje opisuje dinamičku pokretljivost bidisperznih suspenzija koje se sastoje od smjese dviju vrlo različitih tipova čestica. Rezultati pokazuju da amplituda zvučnog vala inducirana primijenjenim električnim poljem nije samo zbroj amplituda valova koje generiraju pojedine čestice, nego veći udjel u ukupnom iznosu pripada većim česticama. Ipak, i utjecaj malih čestica je značajan zbog njihove interferencije u toku fluida i iona oko njih.